Electronic Supplementary Material (ESI) for Journal of Materials Chemistry A.

Supporting Information for:

Facile Synthesis and Characterization of $Bi_{13}S_{18}I_2$ as a Stable Supercapacitor Electrode Material

Keir Adams†, Alba Franco González†, John Mallows, Tianyue Li*, Job Thijssen and Neil Robertson*

School of Chemistry and EaStCHEM, University of Edinburgh, King's Buildings, David Brewster Road, Edinburgh, Scotland EH9 3FJ, UK.

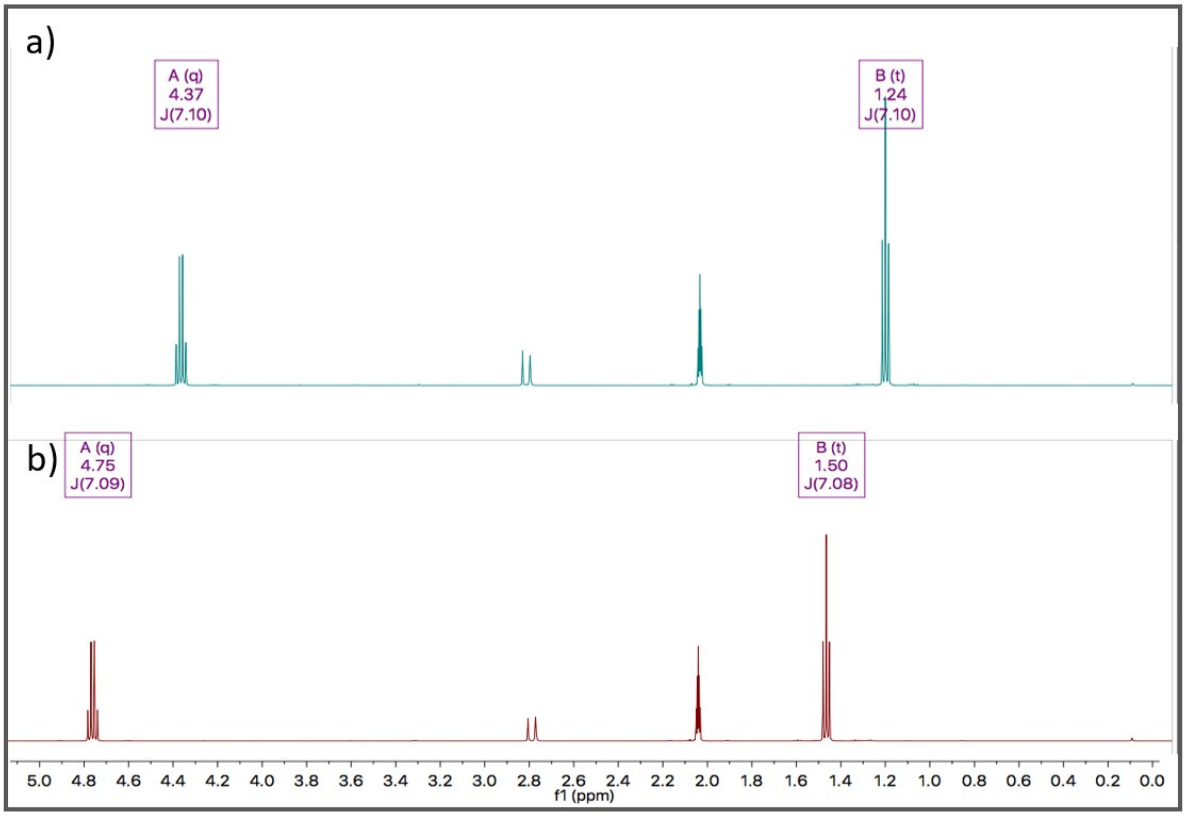

Figure S1. ^1H NMR spectra for (a) $KS_2COC_2H_3$ and (b) $Bi(S_2COC_2H_5)_3$ in deuterated acetone. The additional peaks at 2.0 and 2.8 ppm were identified in literature as H_2O and acetone impurities.[42]

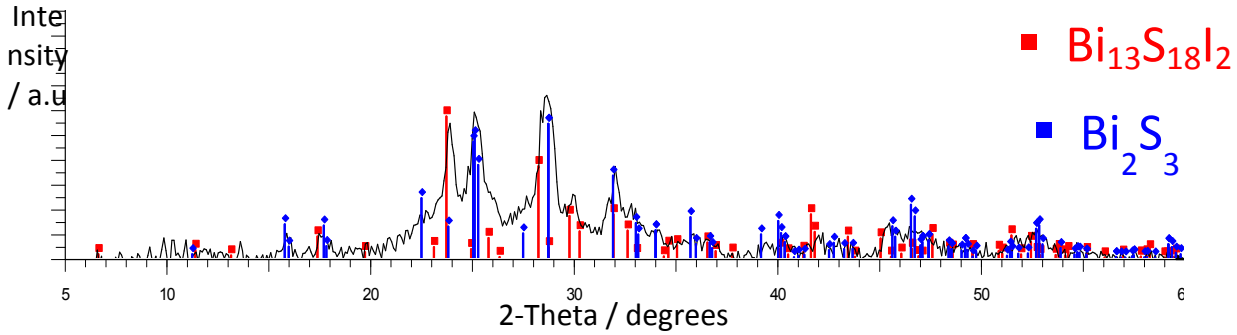

Figure S2. XRD spectra for a thin film synthesized from a precursor solution with a 26:1 $Bi(xt)_3$:BiI_3 ratio, showing patterns corresponding to a mixture of $Bi_{13}S_{18}I_2$ and Bi_2S_3.

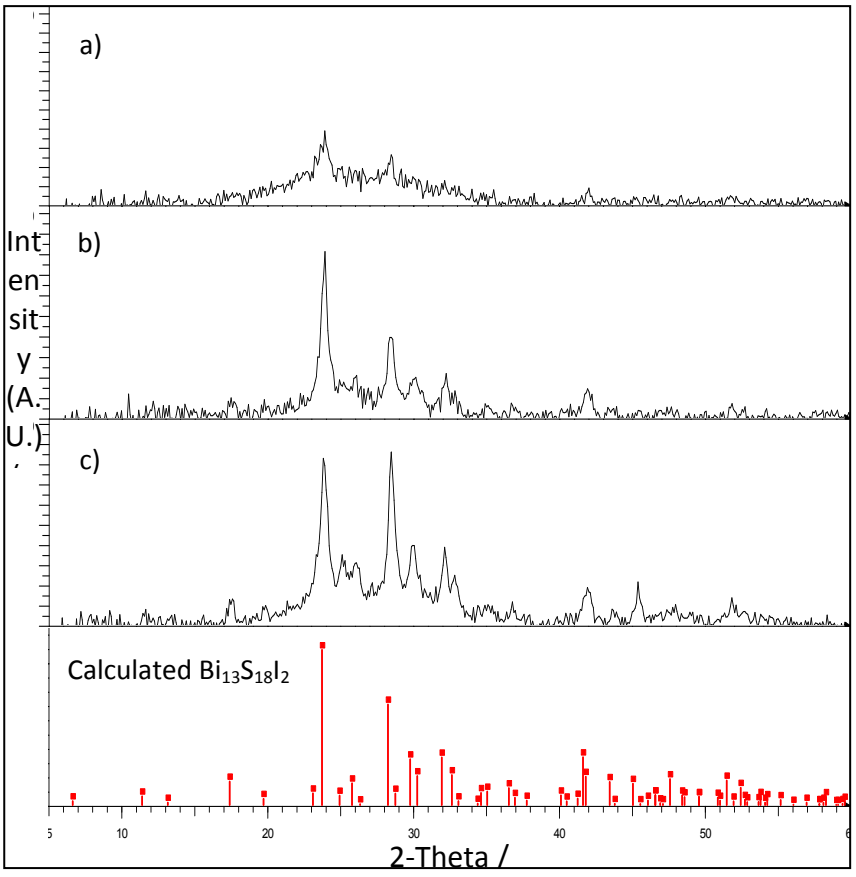

Figure S3. XRD spectra for a thin film comprised of (a) 1 layer, (b) 3 layers, and (c) 5 layers

Table S1 Experimental and reported indirect and direct energy gap for $Bi_{13}S_{18}I_2$

E_g^{ind} / eV	E_g^{dir} / eV	Reference
0.75	0.91	**EXPERIMENTAL**
0.73 ± 0.03	1.08 ± 0.02	[S1]
-	0.825	[S2]
0.30*	0.82 and 0.90	[S3]
-	0.83	[S4]
0.74	**0.89**	**Average**

*Estimated from DFT calculations

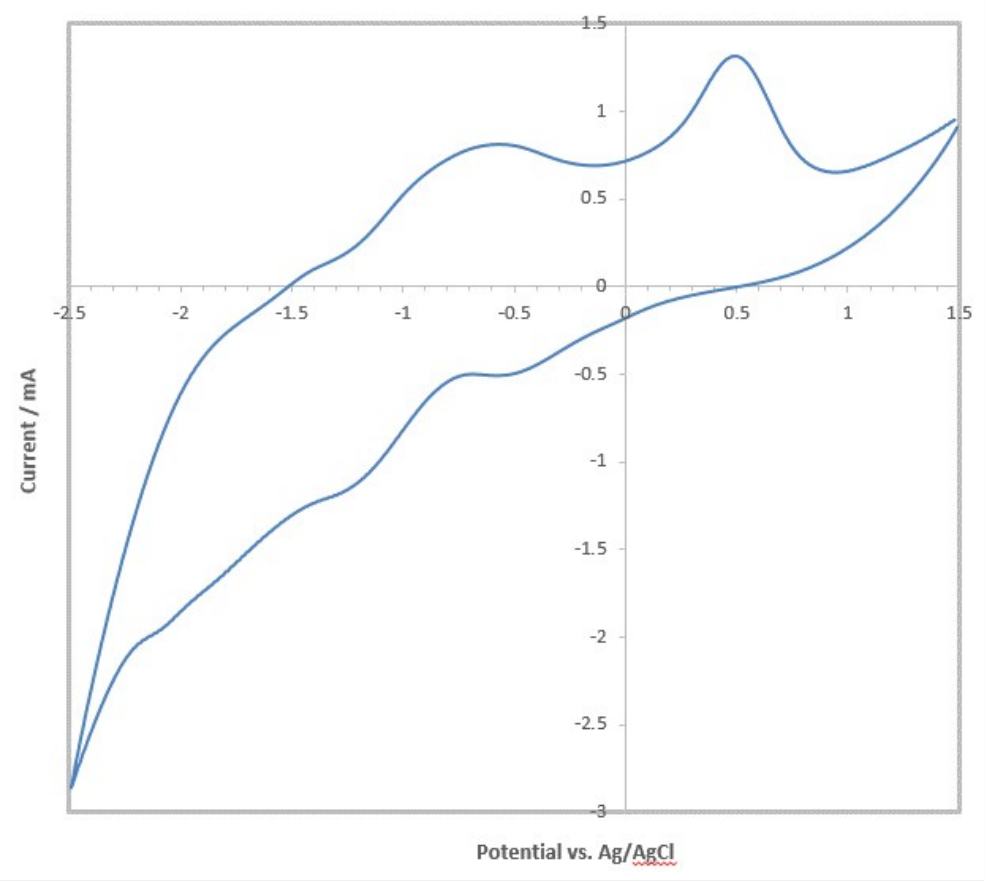

Figure S4. Cyclic voltammogram for $Bi_{13}S_{18}I_2$ thin film sample on mesoporous titania at scan rate of 0.1 V/s

Table S2. (a) Energy density and power density calculated from cyclic voltammetry measurement; (b) Energy density and power density calculated from galvanostatic charge-discharge measurement.

a)

Scan rate / $V \cdot S^{-1}$	0.5	0.2	0.1	0.05	0.02	0.01
Energy Density mWh/kg	478.07	216.6	473.3	782.84	115.74	141.78
Power Density W/kg	30.01	40.23	37.73	28.34	15.62	9.25

b)

Constant Current / $mA \cdot cm^{-1}$	20	10	5	2	1
Energy Density mWh/kg	132.12	161.8	185.8	219.55	254.68
Power Density W/kg	38.67	19.04	9.43	3.76	1.87

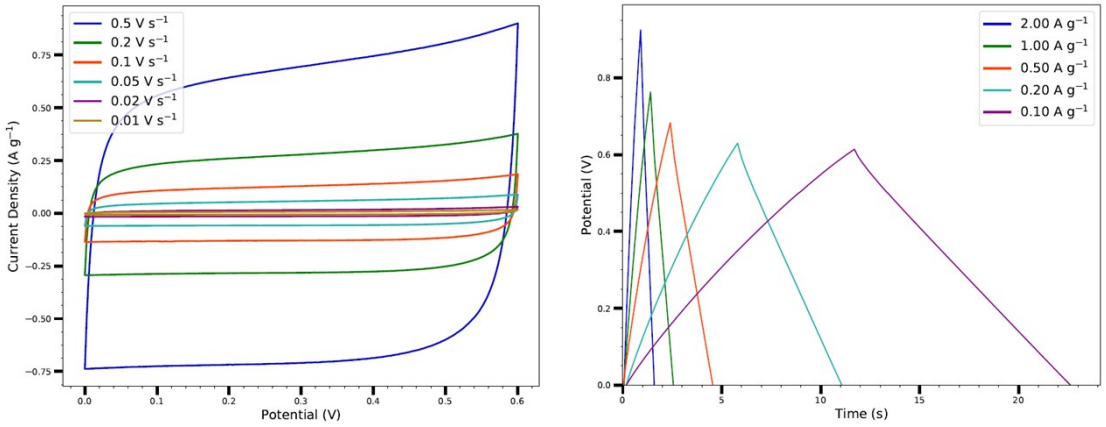

Figure S5. Cyclic voltammograms of the control blank EDLC without active material at varying scan rates. d) Galvanostatic charge−discharge curves of a control blank EDLC device.

Table S3. Areal capacitance and specific capacitance of controlled blank EDLC measured by (a) cyclic voltammetry under different scan rate and (b) galvanostatic charge−discharge under different scan rate

a)

Scan rate / V·S^{-1}	0.5	0.2	0.1	0.05	0.02	0.01
Areal Capacitance/ mFcm^{-2}	1.86	1.88	1.73	1.52	0.97	0.77
Specific Capacitance /Fg^{-1}	0.66	0.67	0.62	0.54	0.34	0.27

b)

current density / A·g^{-1}	2	1	0.5	0.2	0.1
Areal Capacitance/ mFcm^{-2}	2.24	2.26	2.35	2.51	2.64
Specific Capacitance /Fg^{-1}	0.8	0.8	0.84	0.89	0.94

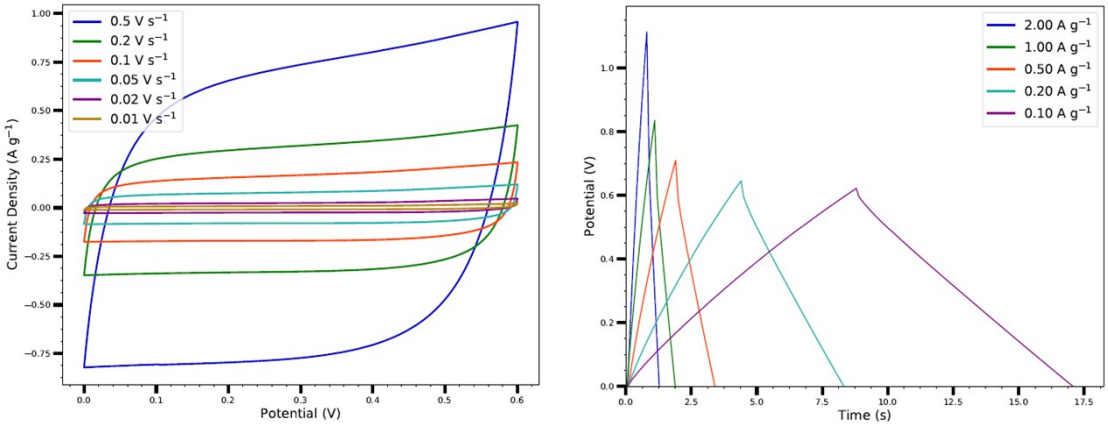

Figure S6 Cyclic voltammograms at varying scan rates (a) and Galvanostatic charge−discharge curves at different constant current (b) of the controlled suspension-deposited $Bi_{13}S_{18}I_2$-based EDLC.

Table S4 Areal capacitance and specific capacitance of controlled suspension-deposited $Bi_{13}S_{18}I_2$-based EDLC measured by (a) cyclic voltammetry under different scan rate and (b) galvanostatic charge−discharge under different scan rate

a)

Scan rate / V*S-1	0.5	0.2	0.1	0.05	0.02	0.01
Areal Capacitance/ mFcm^{-2}	10.33	11.28	11.67	11.07	8.51	5.97
Specific Capacitance /Fg^{-1}	0.7	0.77	0.79	0.75	0.58	0.41

b)

current density / A/g	2	1	0.5	0.2	0.1
Areal Capacitance/ mFcm^{-2}	8.69	9.04	9.63	10.35	10.92
Specific Capacitance /Fg^{-1}	0.59	0.61	0.65	0.7	0.74

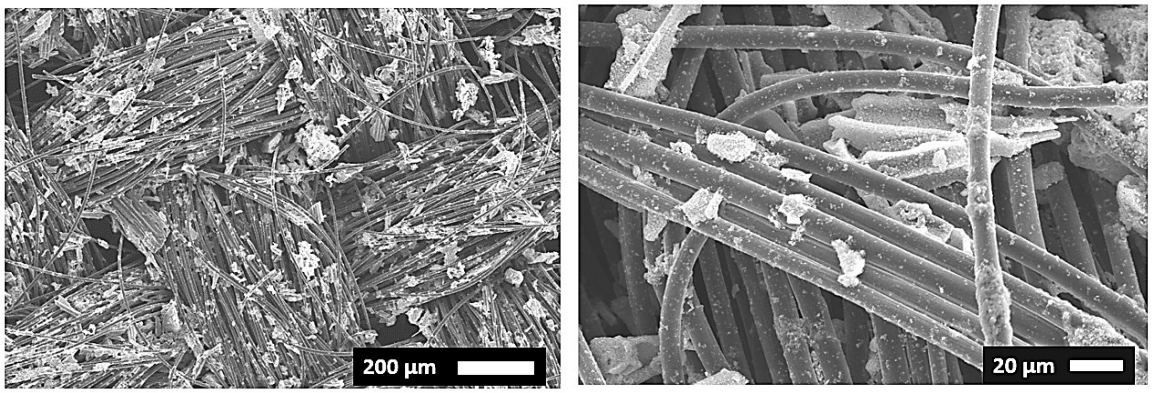

Figure S7. SEM images of $Bi_{13}S_{18}I_2$ electrode prepared from suspension-deposited method

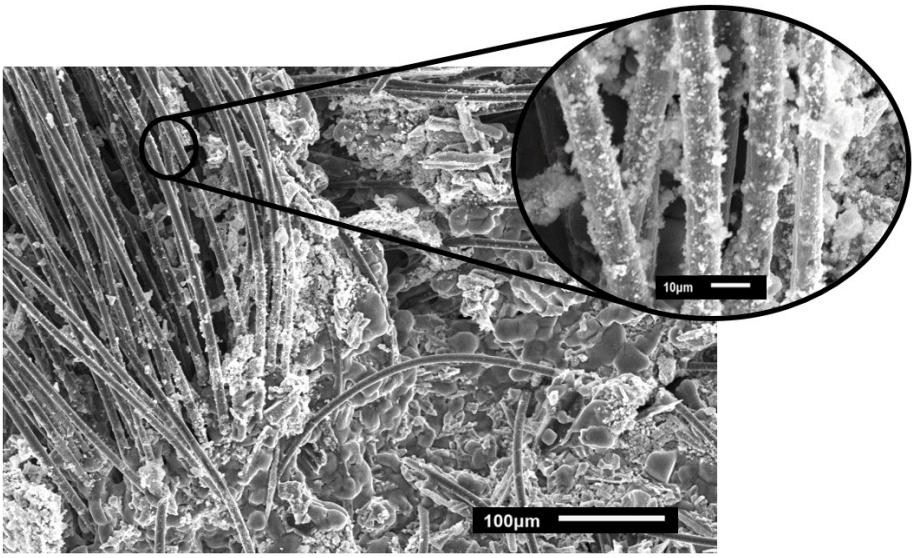

Figure S8. SEM images of $Bi_{13}S_{18}I_2$ electrode after 5000 cycles, with spread-out coverage of active material on carbon fibres. The area with smooth surface coverage indicated the coating from $NaClO_4$ electrolyte.

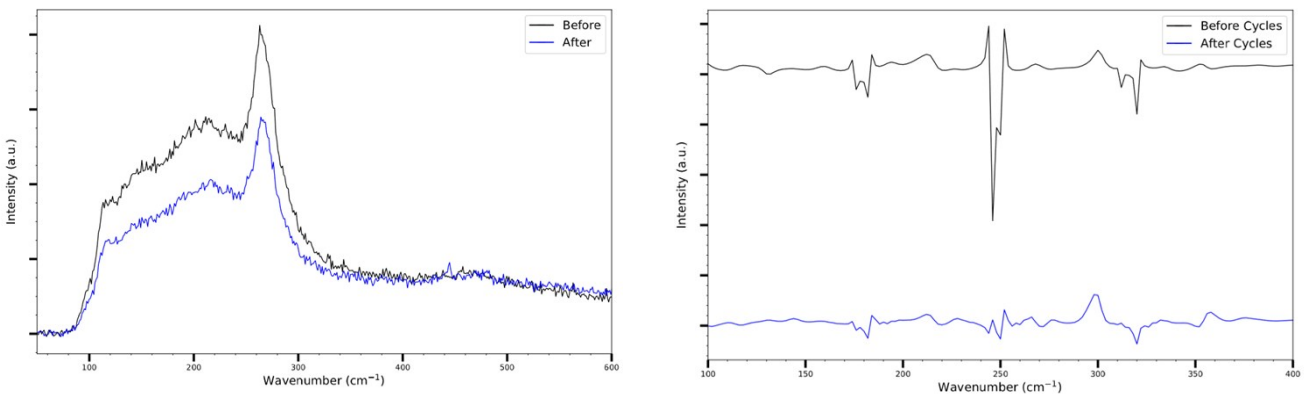

Figure S9. Raman (a) and IR (b) spectra (shifted vertically for clarity) of $Bi_{13}S_{18}I_2$ as electrode material deposited on carbon cloth, compared before and after conducting 5000 cycles of stability test.

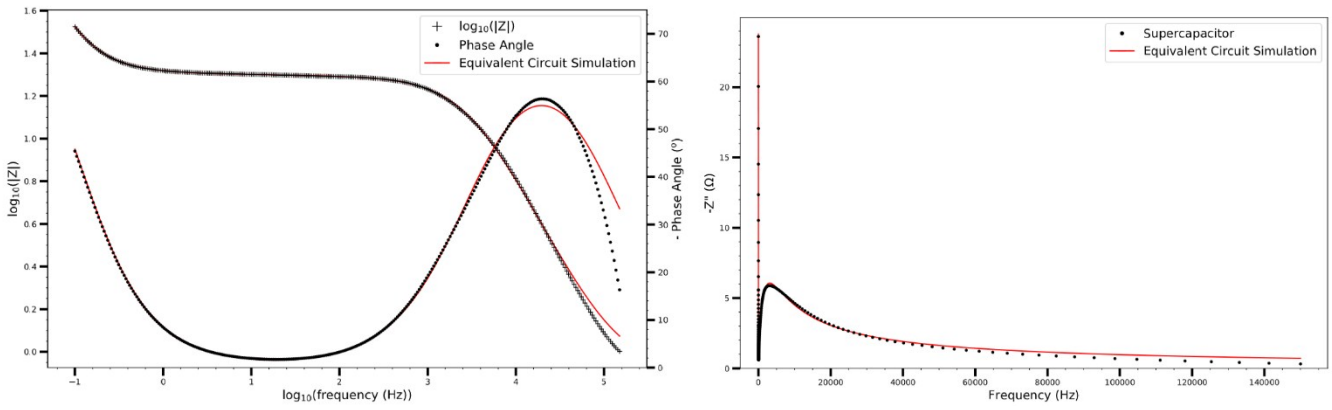

Figure S10. Bode plot (a) and frequency versus out of phase component plot (b) showing both experimental (black) and simulated from equivalent circuit (red).

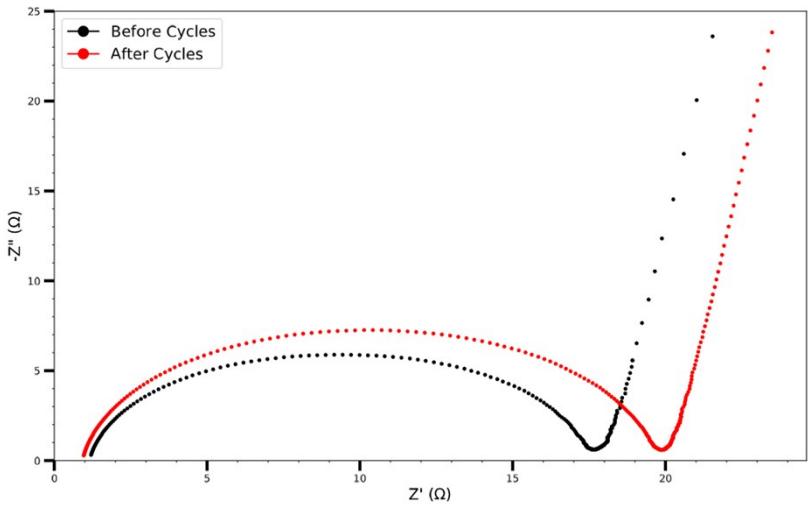

Figure S11. Nyquist plot of $Bi_{13}S_{18}I_2$ EDLC before (black) and after (red) 5000 cycles.

Reference

S1. C.-H. Ho, Y.-H. Chen, Y.-K. Kuo and C. W. Liu, *Chem. Commun*, 2017, **53**, 3741–3744.

S2. Y. Wu, H. Pan, X. Zhou, M. Li, B. Zhou, C. Yang, W.-H. Zhang, J. Jie and C. Li, *Chem. Sci.*, 2015, **6**, 4615–4622.

S3. R. Groom, A. Jacobs, M. Cepeda, R. Drummey and S. E. Latturner, *Chem. Mater.*, 2017, **29**, 3314–3323.

S4. Y. Yan, Y. Xu, S. Lei, X. Ou, L. Chen, J. Xiong, Y. Xiao and B. Cheng, *Dalt. Trans.*, 2018, **47**, 3408–3416.